Feature Line Extraction of Stone Tools Based on Mahalanobis Distance Metric

Shurentsetseg Erdenebayar[1)]   Kouichi Konno[2)]

Graduate School of Engineering, Iwate University

{shurentsetseg} (at)lk.cis.iwate-u.ac.jp

Abstract

Point-cloud-based technique plays a very significant role in 3D model restoration. In the archaeological application of stone tools, the scale drawing, which is hand-drawn from measured stone tools, is traditionally used. In the scale drawing creation, a base drawing which consists outline and ridge lines is initially drawn from geometric features of shape. After that other lines are extracted from knowledge of making stone tools and are added to the base drawing. It requires special knowledge to extract feature lines from stone tools so that scale drawing is time-consuming. Therefore, if the base drawing is automatically extracted, the working hours are reduced. To overcome this issue, this paper proposes a feature line extraction method using the Mahalanobis distance metric. First, the points on outline are extracted from a point cloud. Then, the surface variation is calculated with a various number of neighbors and thus the potential feature points are detected by the analysis of its surface variation. After that, the potential feature points are thinned towards the highest variation points by using Laplacian smoothing. Then, the thinned feature points are shrunk to the potential feature points. Finally, a feature line is extracted by connecting the nearest thinned feature points locating in the Mahalanobis distance field. To verify our method, the extracted feature lines are compared to the ground truth of base drawing drawn by archaeological illustrators. Our method is applied to stone tools, and we confirm the effectiveness of our method.

1 Introduction

In recent years, point clouds are a very popular representation of 3D objects among scientists in the world since higher precision cameras and laser scanners are developed. According to these devices, real objects of any size can be converted into 3D digital data. One of the areas that benefit from point clouds is cultural heritage research. The study of point clouds is contributing to cultural heritage saving for the next generation. One example is the study of stone tool illustrations which is called "Scale Drawing" [1].

A scale drawing is a representation of the shape feature of stone tools. It is generally used in the excavation report in the archaeology area. To publish an excavation report, archaeologists mea-
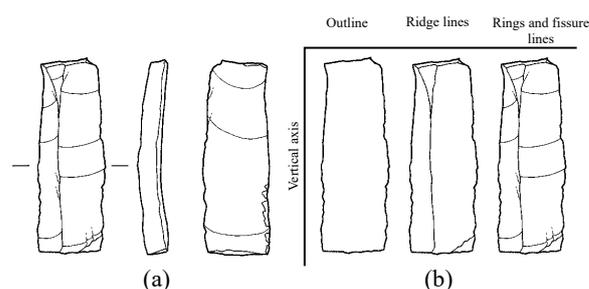

Figure 1: (a) An example of manual scale drawing [2], (b) an example of the steps of the scale drawing

sure stone tools and then make scale drawings by manual operations. However, it is a time-consuming process, and the automatic generation of Scale Drawing is required. In general, scale drawing is represented by four elements, such as

Point cloud

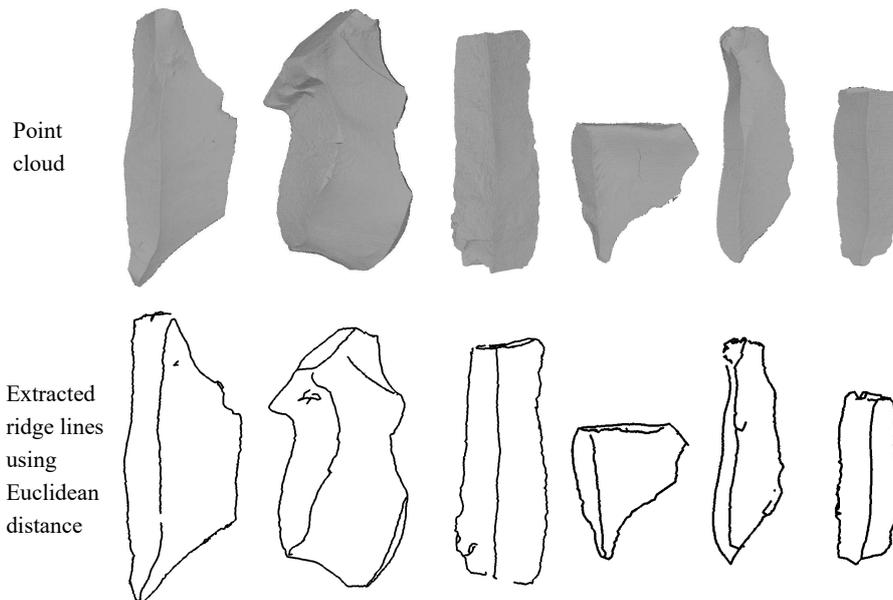Extracted ridge lines using Euclidean distance

Figure 2: Point cloud of stone tools [2] and result of ridge line extraction [3].

outlines, ridge lines, rings, and fissures [1]. Outlines and ridge lines can be extracted from geometric features of the shapes. Rings and fissures have to be investigated from precise observation of specialists and extracted on the knowledge of making stone tools.

Figure 1(a) shows an example of scale drawing from the front, side and back, done by a lithic specialists [2]. Figure 1 (b) shows the steps of making a scale drawing of the stone tool viewed from the front. First, the specialist allocates a drawing area. The longitudinal of a stone tool is drawn along the vertical axis. After that outlines are measured and marked in the sketch. Then outlines are drawn by tracing the measured points. After finishing the outlines, the points on the ridge lines are measured and plotted in the sketch. These points are traced in the same manner. In this paper, the illustration of outline and ridge line calls base drawing. Finally, rings and fissures are added to the base drawing. Making scale drawings from hundreds of stone tools is quite time-consuming. Therefore, efficiency methods are required to reduce time consumption by using point clouds. Outlines and ridge lines are clearer to be extracted and compared to the rings and fissures because these lines are geometric features. On the other hand, to extract rings and fissures require special knowledge of archaeology. Therefore, if outlines and ridge lines are extracted and base drawing is automatically generated, the creation time of scale drawing becomes compressed.

A flake surface is defined by the closed area which is bounded by ridge line. Therefore, all of the flake surfaces are represented by the closed line sequence into the base drawing even if the geometric shape of ridge line may be an ambiguous shape.

There are several techniques to extract feature lines from point clouds [4, 5, 6, 7, 8], while they cannot sufficiently extract feature lines like base drawing. Since a stone tool contains ambiguous shape, closing of flake surface boundary and finding the connection point may be difficult. Therefore, the feature lines to make a base drawing are not sufficiently extracted.

In this paper, a novel feature line extraction method which is expanded by [3] is proposed. The proposed method introduces more flexible distance metric to extract feature lines for a base drawing creation automatically. Our algorithm selects candidate points on feature lines using its dependence on neighbor propagation. Feature lines extracted from a point cloud are evaluated by comparing with for technical hand drawing

and we verify our method has effectiveness.

2 Related works

2.1 Previous study for extracting features

Feature extraction methods have been introduced over the past two decades. Gumhold et al. [7] first formulated curvature using PCA (Principal Component Analysis) for point clouds. Enkhbayar et al. [3] expanded spectral analysis, and they successfully approached the Fast Fourier Transform to estimate the curvature of a point cloud. Then, feature points can be detected by the principal curvature.

Pauly et al. [9, 10] accomplished multi-scale PCA on a point cloud by using an adaptive number of neighborhood points. Due to varying shape of stone tools, a variation of each dimension is suitable to detect potential feature points by using multi-scale PCA. [9, 7, 6] used a minimum spanning tree to construct feature lines. Enkhbayar et al. [3] introduced a line growing technique to construct feature lines. These techniques are calculated in Euclidean space.

In the base drawing, the ridge lines are drawn along the longest sharp edges of stone tools. The detected feature points of such edges have high variation. Therefore, longitudinal connecting along the edges is the best optimization to create the base drawing. Feature points cannot be easily connected depending on variation, because Euclidean distance considers all dimensions have the same variation. Another disadvantage is if there is no feature point to grow in a certain distance, [9, 7, 6] cannot sufficiently construct feature lines. Increasing the connecting radius is not optimal for modifying the feature lines. Figure 2 shows the result of ridge line extraction [3] with principal curvature [11]. When using Euclidean distance, lines cannot be sufficiently extracted and there are gaps between lines.

Today semi-automated illustration system PEAKIT [12] which is used in the archaeological application has introduced in markets. It creates an image illustrating both geometric and archaeological features of stone tools. First features are extracted by openness [12]. Then, extracted fea-
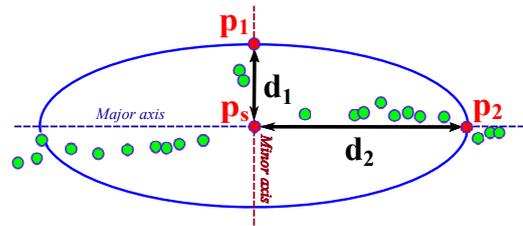

Figure 3: Euclidean distance and Mahalanobis distance

tures are traced by manual operation. Therefore, PEAKIT system still has time complexity. If outlines and ridge lines are extracted and base drawing is automatically generated, the creation time of scale drawing becomes compressed.

2.2 Mahalanobis Distance Metric for Point Clouds

The connection of feature points is hardly required to make a closed area for base drawing creation. For this purpose, our research introduces a Mahalanobis distance metric for constructing feature lines. The Mahalanobis distance metric estimates a distance between two feature points in space for their relevant features. Units in each direction are different because variances in each direction are different. The distribution of points which located the same distance from the center point has a circular or spherical shape in the Euclidean distance metric. Whereas the distribution of points which located the same distance from the center point has ellipse or ellipsoid in the Mahalanobis distance metric, depending on the distribution of the nearby points. Therefore, connecting feature points along the major axis of an ellipse is efficient to extract closed ridge lines.

Figure 3 shows a comparison between the Euclidean distance and the Mahalanobis distance. The ellipse shown in Figure 3 presents the distribution shape of points which are located the same distance from the center point in the Mahalanobis distance metric. In Figure 3, selected point $\mathbf{p}_s$ and its nearest neighbor points $\mathbf{p}_1$ and $\mathbf{p}_2$ are described. According to the Euclidean distance metric, the $\mathbf{p}_2$ is located far from the $\mathbf{p}_s$ compared to the $\mathbf{p}_1$. However, according to the Mahalanobis distance metric, the $\mathbf{p}_1$ and $\mathbf{p}_2$ is

located same distance from the $\mathbf{p}_s$.

Given two data points $\mathbf{p}_i$ and $\mathbf{p}_j$, the Mahalanobis distance can be calculated as follows:

$$d_{i,j}^M = \sqrt{(\mathbf{p}_i - \mathbf{p}_j)^T C^{-1}(\mathbf{p}_i - \mathbf{p}_j)}. \qquad (1)$$

where C^{-1} is the inverse covariance matrix of the selected point set. In this work, a covariance matrix is derived from the projected feature points.

3 Feature extraction

To achieve our goal, three-dimensional features are extracted from the point cloud and the feature lines are constructed using the features.

3.1 Outline Extraction

The outline is extracted first in the same manner as actual scale drawing process. After a viewpoint is set, outline extraction is performed using alphashape of Point Cloud Library.

3.2 Potential Feature Point Detection

A shape of a flake surface is sometimes created by chance with hitting operation. Thus, the shape around ridge lines becomes sometimes ambiguous. Since local surface properties are suitable for detection of potential feature points, surface variation at a point is introduced. In our method, extraction of the potential feature point is based on Pauly et al. [10]. Measured points $\mathbf{x}_i(i = 0, ..., n)$, where i is the index of point $\mathbf{x}_i$ and $n + 1$ is the number of input points, is evaluated by surface variation σ_i^j for point $\mathbf{x}_i$ as

$$\sigma_i^j = \frac{\lambda_0}{\lambda_0 + \lambda_1 + \lambda_2} \qquad (2)$$

where λ_0, λ_1, and λ_2 are the eigenvalues of covariance matrix C with $\lambda_0 \leqslant \lambda_1 \leqslant \lambda_2$ and j is the number of the neighborhood of point $\mathbf{x}_i$. In the experiment, the number of the neighborhood of each point was selected ($j = 10, 20, 30, ..., 200$). Using the surface variation with the different number of the neighborhood has the advantage to reduce the noise.

To detect potential feature points, the surface variation on every point is calculated with the various number of neighbors. After the calculation, every point $\mathbf{x}_i$ obtains a set of surface variations ($\sigma_i^{10}, \sigma_i^{20}, \sigma_i^{30}, ..., \sigma_i^{200}$). If all surface variations σ_i^j are greater than given threshold ε, the point $\mathbf{x}_i$ is determined the potential feature point $\mathbf{p}_y^c$ ($y = 0, ..., m$), where $m + 1$ is the number of potential feature points, as shown in the following Eq.(3). In other words, if above-mentioned condition is satisfied, point $\mathbf{x}_i$ can be noted $\mathbf{p}_y^c$ because of $\mathbf{p}_y^c = \mathbf{x}_i$. Moreover, surface variation σ_i^j of $\mathbf{p}_y^c$ can be noted σ_y^j. Otherwise, that point is not assumed to the potential feature point.

$$\begin{cases} \mathbf{p}_y^c & \text{if all } \sigma_y^j \text{ is satisfied } \varepsilon < \sigma_y^j \\ \mathbf{O} & \text{other} \end{cases} \qquad (3)$$

The sphere radius is used to detect neighboring points in Section 3.2, 3.3 and 3.4. The number of neighbors varies with each point depending on the sphere radius. The sphere radius R is defined by Eq.(4).

$$R = a \cdot \overline{d} \qquad (4)$$

where a is a scale value of iteration and $\overline{d}$ is the average distance [3] between the points shown in Eq.(5).

$$\overline{d} = \frac{1}{n+1} \sum_{i=0}^{n} |\mathbf{x}_i - \mathbf{q}| \qquad (5)$$

where $\mathbf{q}$ is one nearest point of $\mathbf{x}_i$, and $|\mathbf{x}_i - \mathbf{q}|$ is the distance between points $\mathbf{x}_i$ and $\mathbf{q}$.

In this work, each potential feature point $\mathbf{p}_y^c$ is attributed to corresponding surface variation and covariance matrix in order to extracting feature lines. To extract the point which is used for constructing the feature lines, the corresponding surface variation is defined for each potential feature point. To calculate the Mahalanobis distance, the inverse covariance matrix is calculated on each potential feature point.

Since every $\mathbf{p}_y^c$ needs to one corresponding surface variation, the corresponding surface variation of potential feature points $\mathbf{p}_y^c$ is evaluated by the maximum surface variation of a set of surface variations. After the evaluation, every point $\mathbf{p}_y^c$ obtains one corresponding surface variation $\sigma_y^{\max}$.

The second attribute which belongs to $\mathbf{p}_y^c$ is covariance matrix C_y. Firstly the tangent plane at $\mathbf{p}_y^c$ is defined by the normal vector that is derived
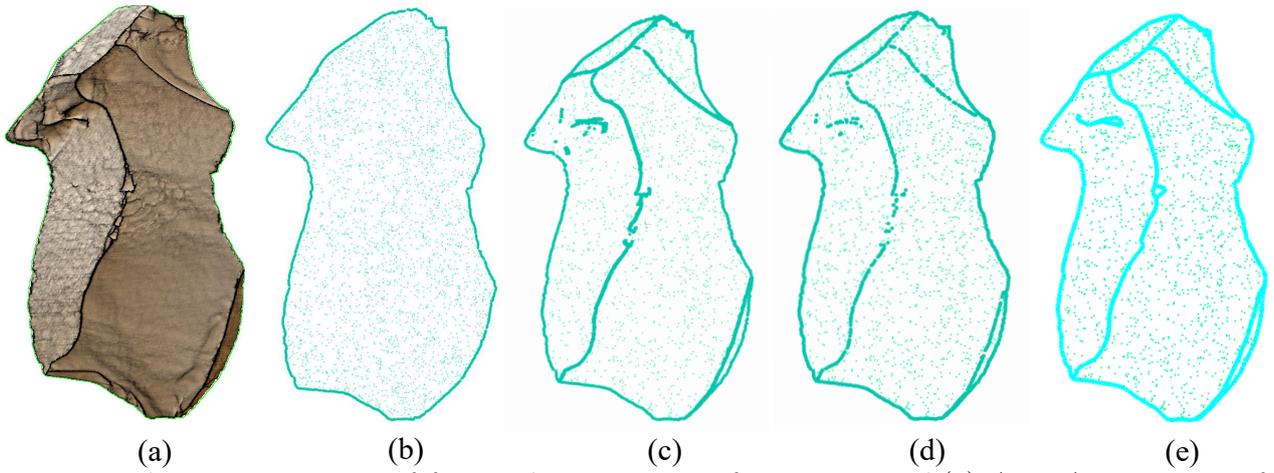
Figure 4: The main structure of feature line extraction for a stone tool:(a) A PEAKIT image of a stone tool [12] (b) extracted outline of the stone tool (c) frontal view of the potential feature points (d) frontal view of thinning feature points after Laplacian smoothing operation (e) frontal view of extracted feature lines based on Mahalanobis distance metric.

by the eigenvector corresponding to the minimum eigenvalue. Then the neighbor potential feature points of $\mathbf{p}_y^c$ are projected onto the tangent plane. Then the covariance matrix is constructed from the projected potential feature points. The covariance matrix C_y at selected potential feature point is defined as:

$$C_y = \frac{1}{k} \sum_{l=1}^{k} (\mathbf{p}_l^c - \overline{\mathbf{p}})^T (\mathbf{p}_l^c - \overline{\mathbf{p}}) \qquad (6)$$

where k is number of neighbor projected potential feature points at $\mathbf{p}_y^c$ when a is equal to 10 and $\overline{\mathbf{p}}$ is the average point of the projected potential feature point set $\mathbf{V}_l(l = 1, ..., k)$ shown in Eq.(7):

$$\overline{\mathbf{p}} = \frac{1}{k} \sum_{l=1}^{k} (\mathbf{V}_l) \qquad (7)$$

Then the inversion of covariance matrix C_i^{-1} is derived.

Figure 4(a) shows a PEAKIT image of a stone tool which is extracted feature line from three-dimensional data of an object by using openness [12], (b) shows the extracted outline of the stone tool. (c) is the potential feature points and (d) shows the result of thinning. Finally, (e) is obtained, which shows the constructed feature lines using the Mahalanobis distance. Detail of thinning process and constructing feature lines are described section 3.3 and 3.4.
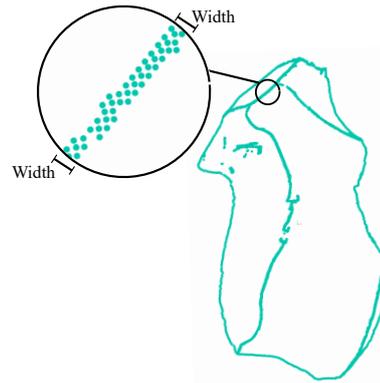

Figure 5: The width example of potential feature points

3.3 Thinning Feature Point

Potential feature points described in Section 3.2 have the width and the density as shown in Figure 5. Since our method to apply potential feature points, the amount of feature points are detected around the sharp edges in Figure 5. To build precise feature lines, some potential feature points are selected to the constructing feature lines. Selecting a number of potential feature points is called the thinning process in this research. The thinning process is evaluated on the only potential feature points. This section describes how to thin potential feature points.

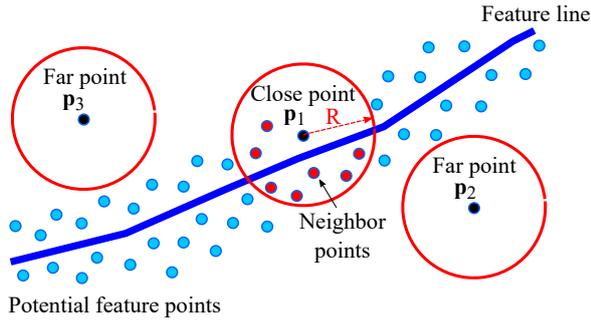To construct feature lines, the potential fea-

Figure 6: The example of the potential feature points.

ture points have to be thinned. For this purpose, all potential feature points are thinned using a surface variation weighted Laplacian smoothing filter.

The ridge points are detected as the potential feature points. However, some potential feature points are extracted far from the real feature lines. Figure 6 shows an example of the far and close potential feature points. If the potential feature point is far from the feature line, the number of neighbors, which is inside of the sphere, is few. On the other hand, if the potential feature points are close to the feature line, the number of neighbors is many.

In the thinning process, some unnecessary feature points can be removed as previous situation. The remaining points that are close to the feature line will be moved closer to the feature lines. The potential feature points are thinned by the following two parts.

Part1: *Remove unnecessary potential feature points*

Step 1. Initialize $a = 5$

Step 2. Calculate number of the neighbor potential feature points v inside the sphere radius R.

Step 3. The potential feature points with less than three neighboring points are removed inside the sphere radius R.

Step 4. If no remove points this process is finished. If it is exist, goto Step 2.

In the second part, some remained potential feature points are selected to the constructing feature lines by the following iteration.

Part2: *Thinning process*

Step 1. Moving to a new position

- Initialize $a = 5$

- Calculate number of the neighbor potential feature points v inside the sphere radius R of $\mathbf{p}_y^c$. Let $\mathbf{Q}_f (f = 1, ..., v)$ be the neighbor potential feature points.

- For the potential feature points $\mathbf{p}_y^c$, a new position $\overline{\mathbf{p}_y^c}$ is calculated by the averaging of the neighbor potential feature points by Eq.(8)

$$\overline{\mathbf{p}_y^c} = \frac{1}{v} \sum_{f=1}^{v} \mathbf{Q}_f \qquad (8)$$

- All potential feature points $\mathbf{p}_y^c$ are moved to the calculated new position $\overline{\mathbf{p}_y^c}$.

Step 2. Obtaining a point with high surface variation

- Initialize $a = 0.5$

- Calculate number of the neighbor potential feature points u inside the sphere radius R of $\mathbf{p}_y^c$. Let $\mathbf{U}_z(z = 1, ..., u)$ be the neighbor potential feature points.

- Create a set $(\sigma_1^{\max}, \sigma_2^{\max}, \sigma_3^{\max}, ..., \sigma_u^{\max})$ of surface variations at each neighbor potential feature point $\mathbf{U}_z$. The corresponding surface variation which is already calculated in the previous section, is used.

- For the potential feature point $\mathbf{p}_y^c$, find the potential feature point which has the highest surface variation from a set of surface variation, as a temporary potential feature point $\mathbf{e}^c$. Figure 7 (a) shows the temporary potential feature point $\mathbf{e}^c$.

- For all potential feature points $\mathbf{p}_y^c$, temporary potential feature points are obtained.
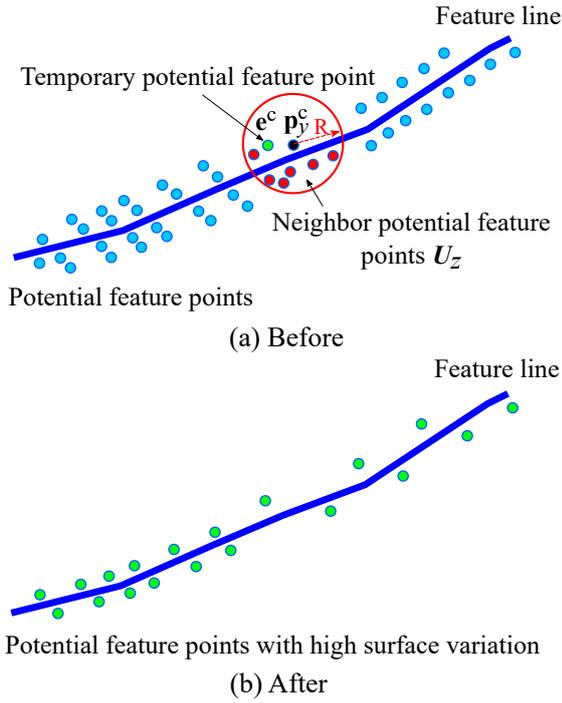
(a) Before

(b) After

Figure 7: The example of selected potential feature points with highest surface variation in neighbor potential feature points

Step 3. Temporary potential feature points are selected as the potential feature points for the Step 4. Other unselected potential feature points are removed. In this step, number of potential feature points will be reduced. Green points in Figure 7 (b) shows obtained potential feature points with high surface variation after this step is finished.

Step 4. If the new potential feature points no longer selected, the process is finished. If it is selected, goto Step 1. Figure 8 shows the example of final potential feature points.

The number of the thinning feature point can be controlled by the parameter of a scale value of iteration.

After the thinning process, the potential feature points are moved. Therefore, the potential feature points are shrunk to the initial position of $\mathbf{p}_y^c$. After the potential feature points are moved, we call these points are thinning feature points $\mathbf{p}_z^r(z = 0, ..., t)$, where $t+1$ is the number of thinning feature points.
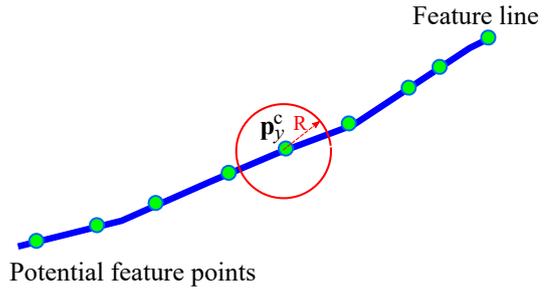

Figure 8: The example of final potential feature points

These extracted thinning feature points are selected to construct the feature lines.

Filtration steps do not significantly affect the position of the real point. Because feature point with the highest surface variation is usually detected on the edges of a stone tool.

3.4 Extraction of Feature Lines

In our method, feature line extraction approach combines a Mahalanobis distance metric algorithm. Feature line construction is not an easy task for stone tools and many approaches have been proposed [13, 14, 15]. However, base drawings cannot be completely connected by using previous works.

To construct feature lines, [13, 14, 15] connect the nearest feature points one by one. As suggested in [3], the feature lines are initialized at the seed points, and arbitrary points obtained by thinning feature points can be chosen as the new seed points. To select a point on the feature line, the nearest thinning feature point should be found sequentially.

This study connects thinning feature points dependent on the variation of neighboring points. Thinning feature points are selected along the principal direction. To find the nearest thinning feature point, the Mahalanobis distance metric evaluates the distances between the current seed point and its nearest thinning feature points. The distances between the current seed point $\mathbf{p}_s$ and the thinning feature points $\mathbf{p}_z^r$ are calculated by Eq. (9).

$$d_{z,s}^M = \sqrt{(\mathbf{p}_z^r - \mathbf{p}_s)^T C_s^{-1} (\mathbf{p}_z^r - \mathbf{p}_s)}. \qquad (9)$$

where the inverse covariance matrix C_s^{-1} is already calculated in the section 3.2. Let $D_e(e = 1, ..., h)$, where h is the number of neighbor thinning feature point, be the Mahalanobis distances of the neighboring thinning feature points at $\mathbf{p}_s$. The nearest distance is found by a sorting algorithm.

The proposed feature line constructing algorithm consists of two steps. At first, feature points are connected to each other by the Mahalanobis distance metric regardless of branch. The initial seed point is selected from the beginning of thinning feature points. The degree of an angle α defined by three points such as the previously selected thinning feature point $\mathbf{p}_{s-1}$, current seed point $\mathbf{p}_s$ and a detected nearest thinning feature point $\mathbf{p}_{s+1}$, is calculated. Figure 9 shows the angle α between the aforementioned thinning feature points. If the α is greater than a given threshold value θ, the detected nearest thinning feature point $\mathbf{p}_{s+1}$ is added to the feature line L. In contrast, the detected angle α is lower than a given threshold value θ, the next nearest thinning feature point $\mathbf{p}_{s+2}$ is checked.

$$L = \begin{cases} \mathbf{p}_{s+1} & \text{if } \alpha \text{ is satisfied } \alpha \geq \theta \\ \mathbf{p}_{s+2} & \text{otherwise} \end{cases} \quad (10)$$

To construct feature lines, the satisfied thinning feature point $\mathbf{p}_{s+1}$ should be selected as a new seed point $\mathbf{p}_s$ based on the Mahalanobis distance.

Second, the distinct feature lines are connected to each other. End points of the distinct feature lines are connected to the nearest feature point located on the nearest feature line by the Mahalanobis distance metric. In the Figure 10, the result of the extracted edges of sample stone tools are shown.

4 Results and limitation

4.1 Experiment Results

This section describes the result from our experiments. The experiments were performed in an Intel Core i7-6700 CPU 3.40 GHz machine with 8GB of RAM and Intel(R) HD Graphics 530. We used the Point Cloud Library (PCL). The input
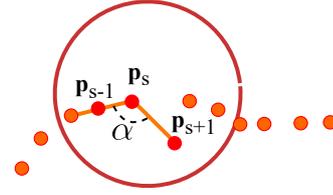

Figure 9: An example of constructing feature line.

data is point data of stone tools obtained by four-directional 3D laser scanners [16].

This paper automatically extracts a base drawing of stone tools. The stone tools are evaluated on the front pose. We tested our proposed method on the six actual stone tools. The extracted base drawings of the stone tools are shown in Figure 10. In this figure, first left column shows the scale drawing and the second column shows the base drawing which is referred to as ground truth. The third column shows the result of the proposed method. To reduce the working hours of creating scale drawing, this paper aims to automatically extract base drawing.

To evaluate the similarity between the ground truth of base drawing and the extracted base drawing, the approximation of pixels are measured [17]. Using the real sizes of the stone tools, the images of the ground truth and the extracted base drawing are quantified by the one-pixel width of 0.1mm. Table 1 shows the number of points, physical properties of the actual stone tools and some evaluation. The similarity of the extracted base drawing and ground truth is defined on the distance 0.5mm.

To define whether the manually created base drawing can be replaced with the automatically extracted scale drawing is possible, extracted base drawing and hand-drawn base drawing are compared quantitatively. To measure the extraction accuracy, F1 score, the harmonic average of the precision and recall (PR), is evaluated in each stone tool data where the F1 score reaches its best value at 1 and worst score at 0. Figure 11 shows the F1 scores of the extracted base drawing for all six stone tools. The best value at 1 of the F1 score indicates that the extracted base drawing is the same as the ground truth, and the extracted base drawing can be reduce working hours of manually creating a base drawing. F1 score takes both
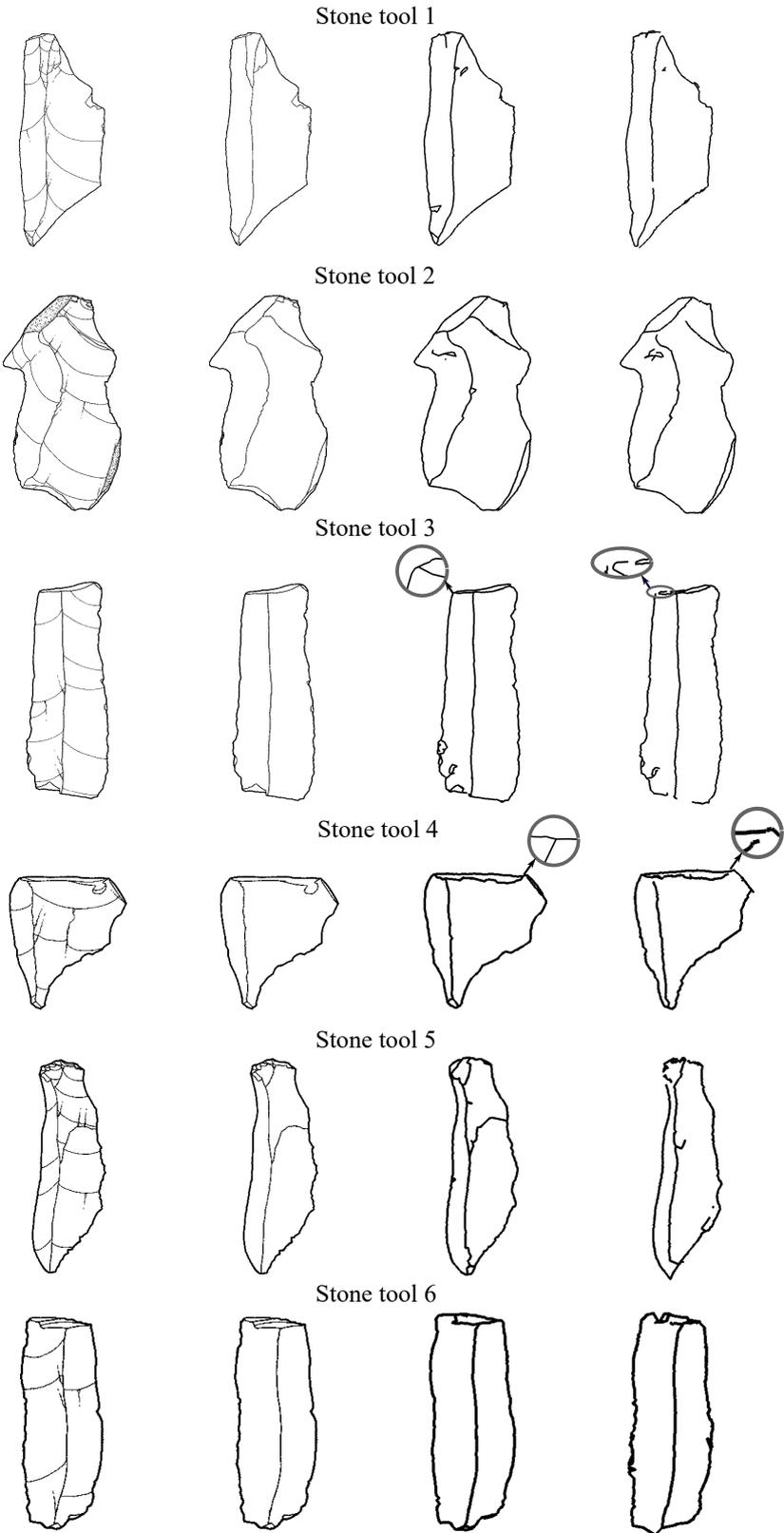
Figure 10: The result of the proposed method. The first left column shows the scale drawings of stone tools, second column shows the ground truth of base drawings, the third column shows the results of the proposed method and fourth column shows the results of the previous work.

Table 1: Physical size of stone tools and evaluations

Measured stone tools	Points	Stone tool sizes			Similarity	Average distance (mm)	F1 score
		Height (mm)	Length (mm)	Width (mm)			
1	174393	80.4	31.8	8.1	83.126	0.403	0.876
2	201679	72.5	44.1	10.8	82.373	0.410	0.899
3	144306	68.0	25.2	7.7	94.885	0.402	0.930
4	46469	29.2	25.6	5.1	87.872	0.397	0.925
5	52913	48.8	15.3	4.2	78.028	0.416	0.813
6	45230	37.2	14.1	4.0	87.343	0.412	0.904
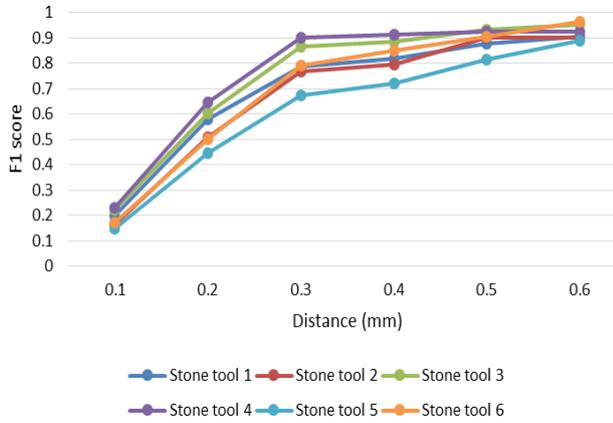
Figure 11: Graph of F1 score of extracted lines.

Figure 12: The unnecessary edges and undetected edges of the results.

false negative and false positive pixels into account. False negative pixels express undetected edges from the ground truth. False positive pixels express unnecessary edges of the extracted base drawing in Figure 12(a).

Moreover, average distance d' is measured by Eq.(11).

$$d' = \frac{\sum_{i=0}^{n} w_i d_i}{\sum_{i=0}^{n} w_i} \qquad (11)$$

where w_i is the overlapped pixel within the distance d_i. The average distance is measured between the distance 0.1mm to 0.6mm within a step 0.1. The result of average distance is shown in Table 1.
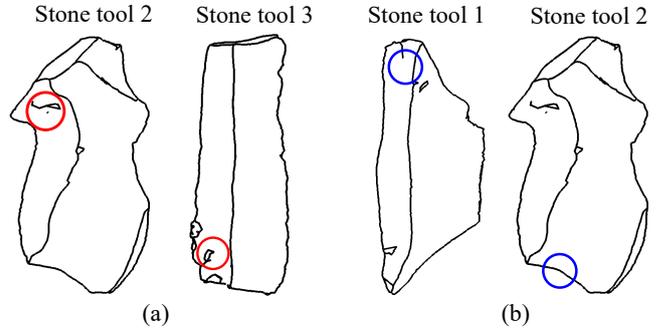
We introduced the comparison of automati-cally extracted base drawing and ground truth images. The base drawing of ground truth is drawn by hand and the proposed base drawing is extracted from the point cloud. When using the Euclidean distance metric, feature lines constructed by the previous method shown in the fourth column of Figure 10 cannot be fully constructed and a lot of gaps between feature lines. Some unconnected edges with hard to see are enlarged in Figure 10. Moreover, some feature lines are unextracted. Our proposed method can extract closed base drawing and the edges are completely connected. Figure 10 shows the result of completely connected edges which is enlarged and cannot be connected by the previous method. In the experiment, the similarities of the stone tools are between 78.028 to 94.885. Our method can properly extract long ridge lines. The average distances of extracted base drawings are between

0.397 to 0.416 in all six stone tools.

4.2 Limitation

Figure 13 shows the types of ridge lines in scale drawing. The limitation of our method is that it is difficult to extract corner small ridge lines of a stone tool. The corner small ridge lines need more specialist knowledge because the shapes around small ridges are ambiguous. The small ridge lines are magnified in Figure 13.

The unnecessary ridge lines are extracted in the stone tools 2 and 3 shown in Figure 12(a) and some referenced ridge lines are not extracted in the stone tool 1 and 2 shown in Figure 12(b). In these cases, extracting ambiguous ridge lines are hardly extracted by the geometric approach. In such a case, an archaeologist may help to extract small ridge lines.
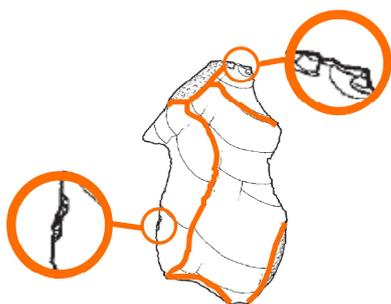

Figure 13: Types of the ridge lines

5 Conclusion

In this paper, a novel method of the extracting base drawing is proposed. The main idea of the method is to select a candidate point of feature lines by its Mahalanobis distance. The advantage of our method is that Mahalanobis distance can reference the covariance of the local neighbor set. For stone tools, the feature lines are usually lined up. In such manner, Mahalanobis distance metric can extract feature lines more properly than Euclidean distance metric for stone tools. In the further research, more precise extraction for small ridge lines are introduced.

The basic concept of our method has already been presented in NICOGRAPH 2017 [11] and this paper extended the concept. We are extremely grateful for lots of efficient advice from the paper reviewers.

Acknowledgments

References

[1] Shinpei Kato and Toshiaki Tsurumaru. *Sekki nyoumon jiten sandoki (in Japanese)*. Kashiwa Shobo Co.,LTD. Tokyo, 1991.

[2] Iwate Cultural Promotion Agency. *Orose Iseki Excavation report (in Japanese))*. 2013.

[3] E. Altantsetseg, Y. Muraki, K. Matsuyama, and k. Konno. Feature line extraction from unorganized noisy point clouds using truncated fourier series. *The Visual Computer*, 29(6-8):617–626, 2013.

[4] J. Daniels II, L. K. Ha, T. Ochotta, and C. T. Silva. Robust smooth feature extraction from point clouds. In *Shape Modeling and Applications, 2007. SMI'07. IEEE International Conference on*, pages 123–136. IEEE, 2007.

[5] J. Daniels II, T. Ochotta, L. K. Ha, and C. T. Silva. Spline-based feature curves from point-sampled geometry. *The Visual Computer*, 24(6):449–462, 2008.

[6] K. Demarsin, D. Vanderstraeten, T. Volodine, and D. Roose. Detection of closed sharp edges in point clouds using normal estimation and graph theory. *Computer-Aided Design*, 39(4):276–283, 2007.

[7] S. Gumhold, X. Wang, and R. S. MacLeod. Feature extraction from point clouds. In *10th International Meshing Roundtable, Sandia National Laboratories*, pages 293–305, 2001.

[8] XF. Pang, MY. Pang, and Z. Song. Extracting feature curves on point sets. *International Journal of Information Engineering and Electronic Business*, 3(3):1, 2011.

[9] M. Pauly, R. Keiser, and M. Gross. Multi-scale feature extraction on point-sampled surfaces. In *Computer graphics forum*, volume 22, pages 281–289. Wiley Online Library, 2003.

[10] M. Pauly, M. Gross, and L. P. Kobbelt. Efficient simplification of point-sampled surfaces. In *Proceedings of the conference on Visualization'02*, pages 163–170. IEEE Computer Society, 2002.

[11] S. Erdenebayar, K. Matsuyama, and K. Konno. Feature line extraction of stone tool based on mahalanobis distance metric. In *NICOGRAPH 2017*, pages 9–16, 2017.

[12] F. Chiba and R. Yokoyama. New method to generate excavation charts by openness operators. In *Proceedings of the 22nd CIPA Symposium, Kyoto, Japan*, volume 1115, pages 15–20, 2009.

[13] T. H. Ho and D. Gibbins. Multi-scale feature extraction for 3d models using local surface curvature. In *Computing: Techniques and Applications, 2008. DICTA'08. Digital Image*, pages 16–23. IEEE, 2008.

[14] X. Pang, Z. Song, and W. Xie. Extracting valley-ridge lines from point-cloud-based 3d fingerprint models. *IEEE computer graphics and applications*, 33(4):73–81, 2013.

[15] L. Yuan, K. Matsuyama, F. Chiba, and K. Konno. A study of feature line extraction and closed frame structure of a stone tool from measured point cloud. In *Nicograph International (NicoInt), 2016*, pages 44–51. IEEE, 2016.

[16] E. Altantsetseg, Y. Muraki, F. Chiba, and K. Konno. 3d surface reconstruction of stone tools by using four-directional measurement machine. *International Journal of Virtual Reality*, 10(1):37–43, 2011.

[17] F. Cole, A. Golovinskiy, A. Limpaecher, H. S. Barros, A. Finkelstein, T. Funkhouser, and S. Rusinkiewicz. Where do people draw lines? *Communications of the ACM*, 55(1):107–115, 2012.

Shurentsetseg Erdenebayar

Shurentsetseg Erdenebayar is a doctor course student at the Graduate School of Engineering, Iwate University from 2016. She received the BE degree in School of Information and Technology, National University of Mongolia in 2007. She received her ME degree in School of Engineering and Applied Sciences, National University of Mongolia in 2014. Her research interest includes geometric modeling and computer graphics. She is a member of The Society for Art and Science.

Kouichi Konno

Kouichi Konno is a professor of Faculty of Engineering at Iwate University. He received a BS in Information Science in 1985 from the University of Tsukuba. He earned his Dr.Eng. in precision machinery engineering from the University of Tokyo in 1996. He joined the solid modeling project at RICOH from 1985 to 1999, and the XVL project at Lattice Technology in 2000. He worked on an associate professor of Faculty of Engineering at Iwate University from 2001 to 2009. His research interests include virtual reality, geometric modeling, 3D measurement systems, and computer graphics. He is a member of Eurographics.